JOURNAL OF PROPULSION AND POWER
Vol. 14, No. 1, January–February 1998

Solar Cell Temperature on Mars

E. Matz,* J. Appelbaum,† and Y. Taitel†
Tel-Aviv University, Tel-Aviv 69978, Israel
and
D. J. Flood‡
NASA Lewis Research Center, Cleveland, Ohio 44135

Missions to the Martian surface will require electric power. Of the several possibilities, photovoltaic power system can offer many advantages. Photovoltaic cell performance increases with decreasing temperatures. The present paper deals with the calculation of the operating temperature of a flexible photovoltaic array needed for the determination of the electric output power from the array. The diurnal temperature variation was determined based on the solution of the heat-balance equation considering radiation, free and forced convection, and conduction. The photovoltaic array was divided into three layers (cover glass, solar cells, and substrate), for which three differential equations were obtained and solved. The solution takes into account the special atmospheric condition prevailing on Mars, considering the diurnal variation of the ambient and surface temperatures, diurnal variation of direct beam, diffuse and albedo irradiances, variation of wind speed, and variation of various Mars atmospheric parameters with temperature.

Nomenclature

al = Mars surface albedo
c_p = specific heat capacity of Mars atmosphere
c_{p1}, c_{p2}, c_{p3} = specific heat of first, second, and third layer, respectively
$E_{i+1,i}$ = heat conduction between layers
F = configuration factor
F^b_{al} = configuration factor of back-side for albedo
F^b_d = configuration factor of back-side for diffuse irradiance
F^b_{grd} = configuration factor of back-side to ground
F^b_{grdb} = configuration factor of back-side to shadowed ground under the photovoltaic array
F^b_{sky} = configuration factor of back-side to sky
F^f_{al} = configuration factor of front-side for albedo
F^f_d = configuration factor of front-side for diffuse irradiance
F^f_{grd} = configuration factor of front-side to ground
F^f_{sky} = configuration factor of front-side to sky
G = solar irradiance on the photovoltaic array plane
G_b = direct beam irradiance
G_{bh} = direct beam irradiance on a horizontal surface
G_{dh} = diffuse irradiance on a horizontal surface
G_0 = reference irradiance
g_m = Mars acceleration gravity
h^b_{free} = free convection heat transfer coefficient for back-side
h^f_{for} = forced convection heat transfer coefficient for front-side
K = thermal conductivity (Mars atmosphere)
K_i = heat conductivity of photovoltaic array layer i
L = flow length (photovoltaic array width, characteristic flow length)
L_i = length (width) of layer i
L_s = aerocentric longitude, position of Mars in orbit around the sun
$L_{x'}$ = fluid flow length (distance from photovoltaic array edge to point of calculation)
m = layer mass
mc_p = heat capacity of the photovoltaic array
m_1, m_2, m_3 = mass of first, second, and third layer, respectively
Nu = Nusselt number
$Nu_{x'}$ = local Nusselt number
P_c = power output, per square meter, of the photovoltaic array at G_0 and T_{ref}
Pr = Prandtl number
Q_h = free and forced convective heat loss
Q_p = electric power output from photovoltaic array
Q_r = radiative heat loss to ground and sky
Q_{sun} = amount of solar energy absorbed
Re = Reynolds number
$Re_{x'}$ = local Reynolds number
T = temperature
T_{amb} = Mars ambient temperature
T_{ambb} = ambient temperature under photovoltaic array
T_{cell} = solar cell temperature
T_{grd} = Mars ground temperature
T_{ref} = solar cell reference temperature
T_{sky} = Mars sky temperature
T_1, T_2, T_3 = temperature of first, second ($T_2 = T_{cell}$), and third layer, respectively
t = time
U = wind speed of Mars atmosphere on the photovoltaic array
$U_{i+1,i}$ = overall heat transfer coefficient between layers $i + 1$ and i
$U_{x'}$ = fluid flow local speed along the photovoltaic array surface
$U_{1,2}$, $U_{2,3}$ = overall heat transfer coefficient between layers, first and second, and second and third, respectively
α = photovoltaic array absorptance
α_b = solar array absorptance, back-side
α_f = solar array absorptance, front-side
α_p = power–temperature coefficient
α_1, α_2, α_3 = absorptance of first, second, and third layer, respectively

Received March 22, 1997; revision received July 20, 1997; accepted for publication July 31, 1997.

*Graduate Student, Department of Electrical Engineering Systems, P.O. Box 39040.
†Professor, Department of Electrical Engineering Systems, P.O. Box 39040.
‡Chief, Photovoltaic and Space Environmental Branch.

β = array inclination angle
ε = photovoltaic array emittance
ε_b = photovoltaic array emittance, back-side
ε_f = photovoltaic array emittance, front-side
θ = sun angle of incidence
μ = viscosity of Mars atmosphere
ρ = density of Mars atmosphere
σ = Stefan–Boltzmann's constant
τ = optical depth of Mars atmosphere

I. Introduction

PHOTOVOLTAICS (PV) provide low-cost power with high reliability and no moving parts. They have powered the space program since Vanguard, and there is every reason to believe they will play a major role in the exploration of Mars, e.g., Mars Pathfinder, July 4, 1997. Photovoltaic cell performance increases with decreasing temperatures, with peak efficiency occurring at 150–200 K; at lower temperatures the efficiency decreases. The purpose of the present study is to calculate the operating temperature of the PV array needed for the determination of its electric power output.

The solar intensity on the surface on Mars is considerably lower than that available in Earth orbit. The average solar intensity at the orbit of Mars is 590 W/m^2, compared with 1368 W/m^2 in Earth orbit. The eccentricity of Mars orbit results in a variation in intensity of about $\pm 19\%$ in the course of a year. Scattering and absorption of light by dust in the Martian atmosphere also decreases the sunlight available.[1–3] Air temperatures were measured by Viking Landers at a height of 1.6 m above the surface over a (Martian) year of measurement, including both local and global dust storms. Viking Lander 1 (VL1) landed at 22.3°N latitude and 47.9°W longitude, and Viking Lander 2 (VL2) landed at 47.7°N latitude and 225.7°W longitude. The air temperature varied from a minimum of 180 K to a maximum of 250 K at VL1, and a 160-K minimum to a maximum of 240 K at VL2. Wind was also measured by the Viking Lander. Average wind speed at the VL2 site was about 2 m/s, with winds of over 17 m/s observed less than 1% of the time. The Mars atmosphere consists of about 95% carbon dioxide and the pressure varies between 6.8 and 10.2 mbar. The season on Mars is indicated by the value of L_s measured in the orbital plane of the planet from its vernal equinox, L_s = 0°; L_s = 0–90° (northern spring), L_s = 90–180° (northern summer), L_s = 180–270° (northern autumn), and L_s = 270–360° (northern winter).

Studies on the temperature calculations of PV arrays were performed for Earth conditions[4–6] or for space.[7] For the first time, in the present study, the operating temperature of solar cells in a flexible PV array was determined from the solution of the heat-balance equation considering radiation, free and forced (wind) convection, and conduction, and taking into account the special atmospheric conditions prevailing on Mars.

II. Heat-Balance Equation

The thermal behavior of a photovoltaic array shown in Fig. 1 may be described by the energy-balance relationship expressed in Eq. (1). The amount of solar energy absorbed by the array is equal to the convective and radiative heat loss to the ambient environment, power converted into electricity, and change in thermal energy content

$$Q_{\text{sun}} = Q_h + Q_r + Q_p + mc_p \frac{\mathrm{d}T_{\text{cell}}}{\mathrm{d}t} \tag{1}$$

Each term in Eq. (1) is a function of several parameters: $Q_{\text{sun}} = f(G, \alpha, \beta, \tau)$; $Q_h = f(T_{\text{cell}}, T_{\text{amb}}, K, L, U, \rho, \mu, Pr, g_m, c_p)$; $Q_r = f(T_{\text{cell}}, T_{\text{sky}}, T_{\text{grd}}, \varepsilon, F)$; and $Q_p = f(Q_{\text{sun}}, T_{\text{cell}})$. First, we will write the heat balance equation for the entire PV array as a lumped mass system. Therefore, we assume no temperature gradients in any direction on the PV array surface and in the perpendicular direction.

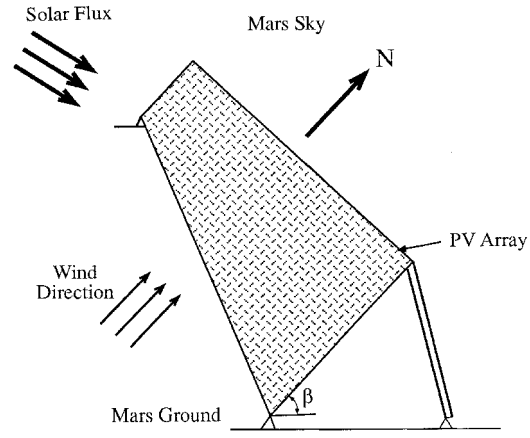

Fig. 1 Photovoltaic array.

A. Solar Energy Absorption

The incident solar irradiance on the front of the PV array consists of the beam, diffuse, and albedo irradiances. The value of each irradiance component depends on the optical depth of Mars' atmosphere.[2] Part of the solar radiation energy is absorbed by the front- and back-side of the PV array, and part is reflected back to the sky and ground. The absorbed solar energy by the front- and back-sides of the PV array is given by

$$Q_{\text{sun}} = \alpha_f G_b \cos\theta + \alpha_f F_d^f G_{\text{dh}} + \alpha_f alF_{\text{al}}^f (G_{\text{bh}} + G_{\text{dh}}) + \alpha_b F_d^b G_{\text{dh}} + \alpha_b alF_{\text{al}}^b (G_{\text{bh}} + G_{\text{dh}}) \tag{2}$$

B. Free and Forced Convection Heat Loss

Both front and back surfaces of open-frame-mounted PV arrays are exposed to ambient air. In the heat-balance equation we consider wind cooling. Forced convection of wind over the PV array involves a large number of variables such as wind speed, wind direction, PV array inclination angle, etc. We assume in our calculations a south–north wind direction coinciding with the south-facing PV array. Therefore, the front-side of the array is subject to forced convection. We also assume that the back-side is subject to free convection, and in case of an elevated array, the turbulence may be neglected. The convection heat loss is therefore given by

$$Q_h = h_{\text{for}}^f (T_{\text{cell}} - T_{\text{amb}}) + h_{\text{fre}}^b (T_{\text{cell}} - T_{\text{amb}\,b}) \tag{3}$$

A reasonable assumption is $T_{\text{amb}} = T_{\text{amb}\,b}$, because the back-side is open to the ambient atmosphere and elevated from the ground (Fig. 1).

C. Radiative Heat Loss

Radiative heat transfer between the PV array and the environment may be affected by sky and ground temperatures and the shadowed ground temperature under the array, as well as by configuration factors:

$$Q_r = \varepsilon_f \sigma F_{\text{sky}}^f (T_{\text{cell}}^4 - T_{\text{sky}}^4) + \varepsilon_f \sigma F_{\text{grd}}^f (T_{\text{cell}}^4 - T_{\text{grd}}^4) + \varepsilon_b \sigma F_{\text{sky}}^b (T_{\text{cell}}^4 - T_{\text{sky}}^4) + \varepsilon_b \sigma F_{\text{grd}}^b (T_{\text{cell}}^4 - T_{\text{grd}}^4) + \varepsilon_b \sigma F_{\text{grd}\,b}^b (T_{\text{cell}}^4 - T_{\text{grd}\,b}^4) \tag{4}$$

D. Electric Power of PV Array

The electric power output of the PV array depends on the incident irradiance and solar cell temperature. Assuming that the power output depends linearly on the incident irradiance and decreases with temperature, one may write the electric power output per square meter of PV array as

$$Q_p = (G/G_0) P_c [1 - \alpha_p (T_{\text{cell}} - T_{\text{ref}})] \tag{5}$$

The heat balance equation may now be expressed in its differential form by different components [Eqs. (2–5)], as

$$mc_p \frac{dT_{cell}}{dt} = \alpha_f G_b \cos\theta + \alpha_f F^f_d G_{dh} + \alpha_f alF^f_{al}(G_{bh} + G_{dh}) + \alpha_b F^b_d G_{dh} + \alpha_b alF^d_{al}(G_{bh} + G_{dh}) - (G/G_0)p_c[1 - \alpha_p(T_{cell} - T_{ref})] - h^f_{for}(T_{cell} - T_{amb}) - h^b_{fre}(T_{cell} - T_{amb\,b}) - \varepsilon_f\sigma F^f_{sky}(T^4_{cell} - T^4_{sky}) - \varepsilon_f\sigma F^f_{grd}(T^4_{cell} - T^4_{grd}) - \varepsilon_b\sigma F^b_{sky}(T^4_{cell} - T^4_{sky}) - \varepsilon_b\sigma F^b_{grd}(T^4_{cell} - T^4_{grd}) - \varepsilon_b\sigma F^b_{grd\,b}(T^4_{cell} - T^4_{grd\,b}) \quad (6)$$

E. Photovoltaic Array — Three-Layer Model

The PV array is composed of glass, encapsulants, solar cells, intercell spaces, and substrates. The PV array may also be treated as a multilayer model for which a separate heat balance equation may be written for each layer. Consequently, this approach will result in a better estimation of the solar cell temperature.

We have divided the PV array into three layers: the first layer is a cover glass transparent to solar radiation; the second layer consists of the solar cells and electric interconnections; and the third layer is the substrate. The mechanism of heat transfer of the PV array may be described as follows: The first transparent layer transmits most of the solar flux to the second layer (solar cells). A large part of solar flux reaching the solar cells is absorbed and another part is reflected back through the first transparent layer to the atmosphere. The first layer convects heat to the ambient and radiates heat to the sky and ground. The back surface of the first layer conducts heat to the solar cell layer (second layer). The second layer conducts heat to the first and third layers. The back surface convects heat to the ambient and radiates heat to the sky, ground, and the shadowed ground under the PV array. The mechanism of the heat transfer of the PV array described by the three layers is shown in Fig. 2 and is given by the following three differential time-dependent equations:

$$m_1c_{p1}\frac{dT_1}{dt} = \alpha_1[G_b\cos\theta + F^f_d G_{dh} + alF^f_{al}(G_{bh} + G_{dh}] - \varepsilon_1\sigma F^f_{sky}(T^4_1 - T^4_{sky}) - \varepsilon_1\sigma F^f_{grd}(T^4_1 - T^4_{grd}) - h^f_{for}(T_1 - T_{amb}) + U_{1,2}(T_2 - T_1) \quad (7a)$$

$$m_2c_{p2}\frac{dT_2}{dt} = \alpha_2[G_b\cos\theta + F^f_d G_{dh} + alF^f_{al}(G_{bh} + G_{dh})] - U_{1,2}(T_2 - T_1) - U_{2,3}(T_2 - T_3) - Q_p \quad (7b)$$

$$m_3c_{p3}\frac{dT_3}{dt} = \alpha_3[F^b_d G_{dh} + alF^b_{al}(G_{bh} + G_{dh})] - h^b_{fre}(T_3 - T_{amb\,b}) - \varepsilon_3[\sigma F^b_{sky}(T^4_3 - T^4_{sky}) - \sigma F^b_{grd}(T^4_3 - T^4_{grd}) - \sigma F^b_{grd\,b}(T^4_3 - T^4_{grd\,b})] + U_{2,3}(T_2 - T_3) \quad (7c)$$

III. Parameters of Heat Balance Equation

The parameters needed for solving the heat balance equations [Eqs. (7a–7c)] will now be determined and some results will be given in this section for two periods $L_s = 141°$ (Martian summer with clear skies) and $L_s = 284°$ (Martian winter at time of dust storm) both at the location of VL1.

A. Radiative Heat Loss

1. Sky Temperature

The equations for sky temperature in the literature[4,8] refer to Earth where the atmosphere is much more dense than Mars (8 mbar). The temperature for Mars in this study is based on the general circulation model and the radiative transfer equation for Mars[9] and the infrared flux emitted from the Martian sky. The sky effective temperature was evaluated using flux data assuming the sky is a blackbody. The variation of sky temperature for $L_s = 141°$ and $L_s = 284°$ is shown in Figs. 3a and 3b, respectively.

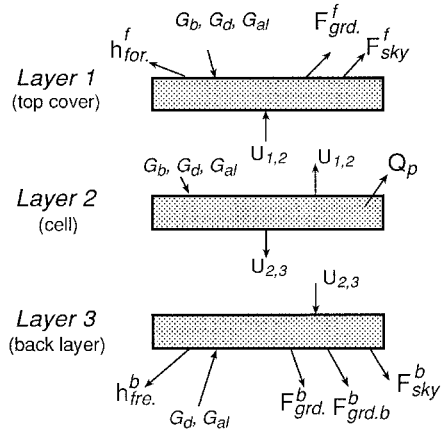

Fig. 2 Mechanism of heat transfer of three-layer PV array.

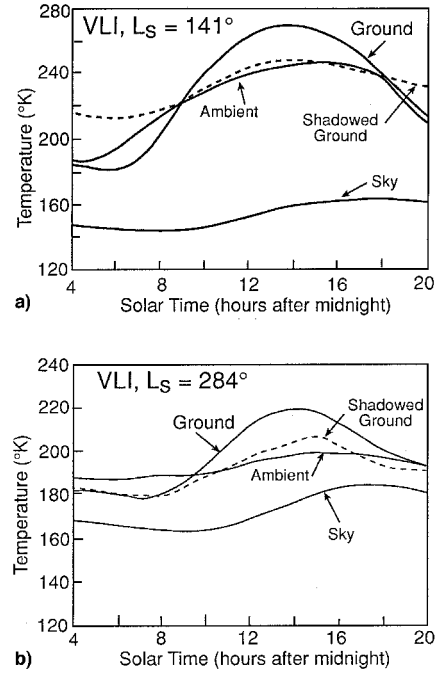

Fig. 3 Variation of sky, ground, shadowed-ground, and ambient temperatures for a) $L_s = 141°$ and b) $L_s = 284°$.

2. Ground Temperature

Ground temperature on Mars surface was derived from the Viking infrared thermal mapping (IRTM), processed by Kieffer.[10] However, for the calculation of solar cell temperature, one needs the diurnal variation of the ground temperature. Again, this information is based on Haberle.[8,9] Figures 3a and 3b describe the variation of ground temperature for $L_s = 141°$ and $L_s = 284°$ at VL1.

3. Shadowed Ground Temperature

Ground temperature in the shadow may be derived from Viking's temperature sensors,[11] although difficulties in measuring the temperature occurred and the data are quite limited. Figures 3a and 3b give these temperatures for $L_s = 141°$ and $L_s = 284°$ at VL1.

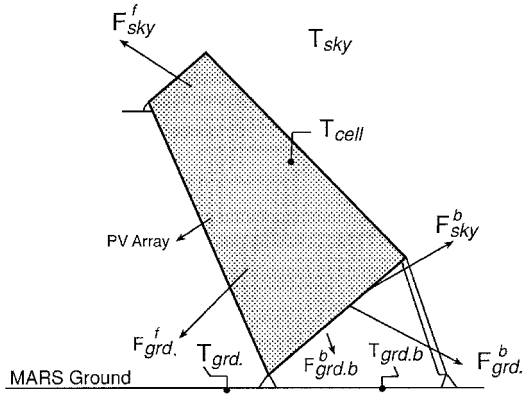

Fig. 4 Configuration factors of PV array for the calculation of radiation heat transfer.

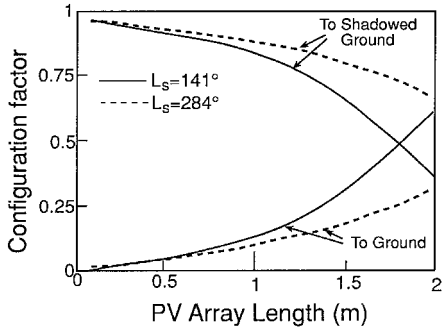

Fig. 5 Variation of the configuration factor for the PV array, back-side to the ground and back-side to the shadowed ground for L_s = 141° and L_s = 284°.

4. Ambient Temperature

Ambient temperatures were measured by Viking Landers at 1.6 m above the ground. Again, the variation of the ambient temperature for L_s = 141° and L_s = 284° at VL1 is given in Figs. 3a and 3b, respectively.

5. Configuration Factors

The configuration factors involved in the radiation heat transfer calculation are shown in Fig. 4. The configuration factors of the front-side to the sky and the front-side to the ground are given by[8]

$$F^f_{\text{sky}} = (1 + \cos\beta)/2, \qquad F^f_{\text{grd}} = (1 - \cos\beta)/2 \tag{8}$$

The back-side of the PV array radiates heat to the sky, exposed ground, and the shadowed ground under the PV array. The calculation of the configuration factor of the back-side to the shadowed ground $F_{\text{grd}\,b}$ is more complicated because it varies with the array height. A special computer program was developed for this purpose. The following relation may be applied for each point on the back-side:

$$F^b_{\text{sky}} + F^b_{\text{grd}} + F^b_{\text{grd}\,b} = 1 \tag{9}$$

where F^b_{sky} is constant for the back-side and is $F^b_{\text{sky}} = F^f_{\text{grd}}$. Figure 5 shows the configuration factors for the back-side to the ground and to the shadowed ground for L_s = 141° and L_s = 284° at VL1. The configuration factor of the back-side to the shadowed ground varies with the shadowed area under the PV array and it varies with the season (L_s). The configuration factors of the front- and back-sides for the diffuse radiation and the albedo needed for Eqs. (7) are

$$F^f_d = F^f_{\text{sky}}, \quad F^f_{\text{al}} = F^f_{\text{grd}}, \quad F^b_d = F^b_{\text{sky}}, \quad \text{and} \quad F^b_{\text{al}} = F^b_{\text{grd}} \tag{10}$$

B. Convection Heat Loss

Both front- and back-sides of the PV array convect heat to the surrounding; the front-side by forced convection and the back-side by free convection.

1. Forced Convection Heat Transfer Coefficient

The forced heat transfer coefficient was determined taking into account the wind velocity measured by the Viking Landers[12] and under the following assumptions:

1) The wind speed is taken in the south–north direction coinciding with the south-facing PV array (Fig. 6), and its magnitude is the resultant in both south–north and west–east directions.

2) The wind fluid (atmosphere) flow on the array surface is laminar (verified by Reynolds number).

The local forced heat transfer coefficient between the array surface and the wind fluid is given by Chapman[13]:

$$h_{\text{for}} = N_{ux'}K/L_{x'} \tag{11}$$

where

$$Nu_{x'} = 0.33Re^{1/2}_{x'}Pr^{1/3} \tag{12}$$

$$Re_{x'} = U_{x'}L_{x'}\rho/\mu \tag{13}$$

To determine the local Reynolds number, it is necessary to calculate the variation of the wind speed on the inclined PV array. This is obtained by solving the general Laplace equation for fluid potential in a defined flowfield. Figure 7 describes the variation of the local wind speed along the front surface of the PV array for L_s = 141° and L_s = 284° at the VL1 location based on the measured wind speed U = 7.6 m/s and U = 9.5 m/s, respectively. The local forced heat transfer coefficient $h^f_{\text{for}\,x'}$ may now be calculated. The results are shown in Fig. 8 for L_s = 141° and L_s = 284°.

2. Free Convection Heat Transfer Coefficient

The back-side of the PV array dissipates heat by free convection. The free heat transfer coefficient depends on many parameters and was calculated based on Chapman[13] for an in-

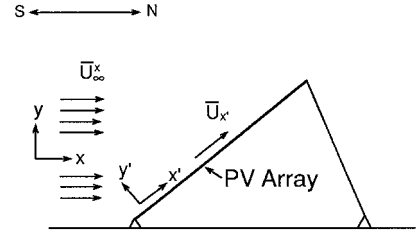

Fig. 6 Wind direction before and along the PV array.

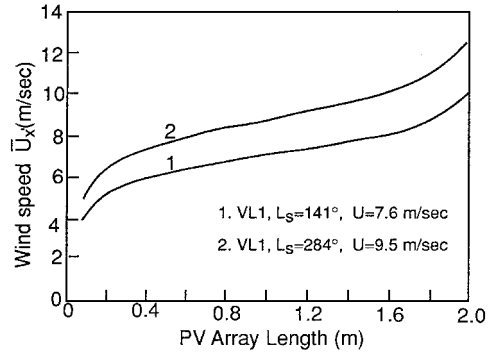

Fig. 7 Variation of local wind speed along the front surface of the PV array for L_s = 141° and L_s = 284°.

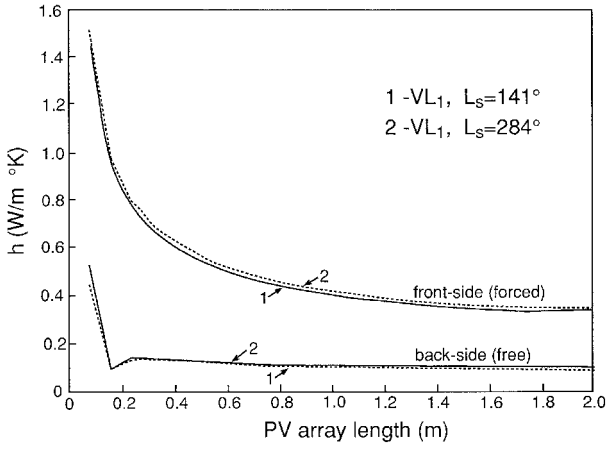

Fig. 8 Variation of forced $h^f_{\text{for},x'}$ and free h^b_{free} heat transfer coefficients for front and back-sides along the PV array, respectively, for L_s = 141° and L_s = 284°.

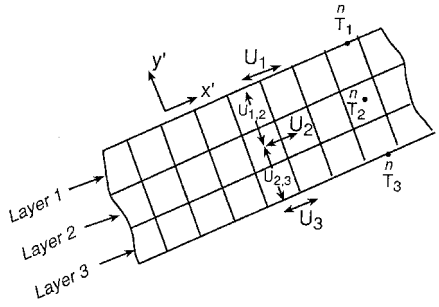

Fig. 9 Conduction along and between layers of the PV array.

clined surface involving local Nusselt, Grashof, and Reynolds expressions. The variation of h^b_{fre} is shown in Fig. 8.

C. Heat Conduction

Heat is conducted between layers in the y' direction of the PV array (Fig. 9), as a result of temperature differences between the front- and the back-sides of the PV array. In addition, there is heat conduction in the x' direction along the array layers resulting from the variations of convective heat transfer coefficient and the back-side configuration factors for radiation. The heat conduction between two layers i and $i + 1$ in the y' direction is given by

$$E_{i+1,i} = U_{i+1,i}(T_{i+1} - T_i) \tag{14}$$

where

$$U_{i+1,i} = \frac{1}{L_{i+1}/K_{i+1} + L_i/K_i} \tag{15}$$

The heat conduction in a given layer, i, of the PV array at two different points, n and $n - 1$, in the x' direction is given by

$$\overset{n}{E}_i = U_i(\overset{n}{T}_i - \overset{n-1}{T}_i) \tag{16}$$

where

$$U_i = \frac{1}{L_n/K_i} \tag{17}$$

and L_n is the layer increment length between points n and $n - 1$.

D. Thermodynamic Parameters of Mars Atmosphere

Several parameter values of Mars' atmosphere are needed for solving the heat-balance equation.

Table 1 Absorptance and emittance of the three-layer PV array

Solar array layers	α	ε
1. Cover glass	0.024	0.86
2. Solar cell	0.64	——
3. Substrate	0.28	0.86

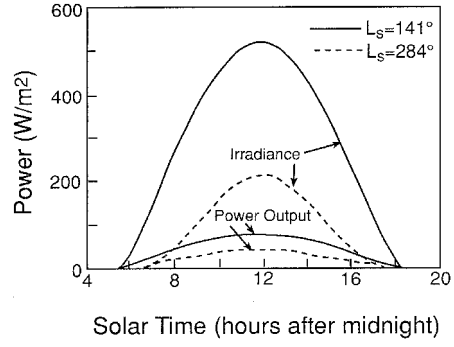

Fig. 10 Variation of global irradiance incident on the PV array and PV array output power for L_s = 141° and L_s = 284°.

Mars' atmosphere consists of about 95% carbon dioxide. The atmospheric pressure varies between about 6.8 and 10.2 mbar; therefore, it may be assumed that the atmospheric gas obeys the law of ideal gases, thus obtaining the specific weight $\rho = 0.018$ kg/m^3 for 8.5 mbar of CO_2 [see Eq. (13)].

The dynamic viscosity μ of an ideal gas depends on its temperature and is almost independent of its pressure. The dynamic viscosity [Eq. (13)] for CO_2 varies between 0.94×10^{-5} and 1.54×10^{-5} kg/m s for a variation in temperature between 180 and 300 K.[14]

The thermal conductivity K of CO_2 depends on the temperature and only weakly on pressure. The thermal conductivity [Eq. (11)] varies between 8.3×10^{-3} and 16.2×10^{-3} W/m K for the temperature range of 180–300 K.[14]

The Prandtl number P_r depends weakly on temperature and is almost independent of pressure. The Prandtl number [Eq. (12)] was determined based on Ref. 14 and is about 0.8 for a temperature range between 180 and 300 K.

E. PV Array Thermal Parameters

The absorptance α and emittance ε for the flexible PV array were determined by taking into account the dependence of the absorptance on wavelength for the solar cells and the substrate layers. Table 1 gives the values for α and ε for the three-layer array. The substrate absorptance of 0.28 is for light incident from the back. Table 2 gives the thermal conductivity, specific heat capacity, and density of the three layers, taking into account the adhesives, conductors, and the flexible printed-circuit relative volumes and their thermal properties.

F. PV Array Power Parameters

The power output of the silicon solar cells refers to cell parameters [Eq. (5)] at a reference irradiance of G_0 = 1368 W/m^2 air mass zero (AMO), at a T_{ref} of 298 K, a PV array output power of 175 W/m^2 at G_0 and T_{ref}, and a power-temperature coefficient of α_p = 4.5%/K. The variation of the global irradiance incident[1–3] on the PV array surface and PV array output power for L_s = 141° and L_s = 284° is shown in Fig. 10 for a β of the array equal to the latitude at VL1.

IV. Operating Temperature of PV Array on Martian Surface

The solution of the heat-balance equations [Eqs. (7)] resulted in the operating temperature of the solar cells on the Martian surface. Figure 11 shows the diurnal variation of the

Table 2 Thermal conductivity, specific heat capacity, and specific weight of the three-layer PV array

Solar array	K, W m^{-1} K^{-1}	c_p, J kg^{-1} K^{-1}	ρ, kgm^{-3}	Thickness, m
1. Cover glass	0.66	824	2400	0.2×10^{-3}
2. Solar cells	137.95	476	2850	0.33×10^{-3}
3. Substrate (Kapton)	0.4	1506	1580	0.089×10^{-3}

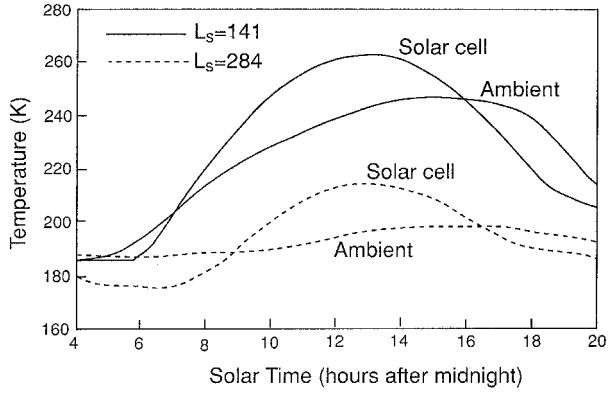

Fig. 11 Diurnal variation of solar cell and ambient temperature for L_s = 141° and L_s = 284° at solar times 11:00 and 12:00.

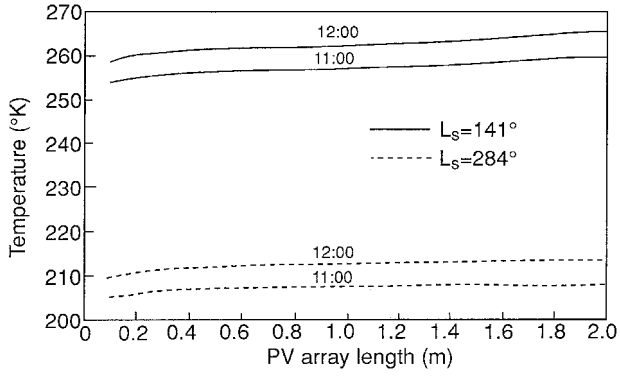

Fig. 12 Variation of solar cell temperature along the PV array for L_s = 141° and L_s = 284° at solar time 11:00 and 12:00.

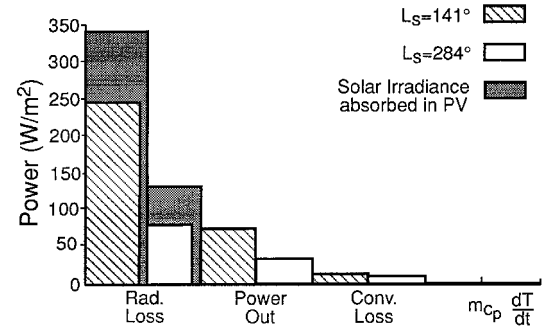

Fig. 13 Division of heat-balance equation components of the PV array for L_s = 141° and L_s = 284° at 12:00 solar time.

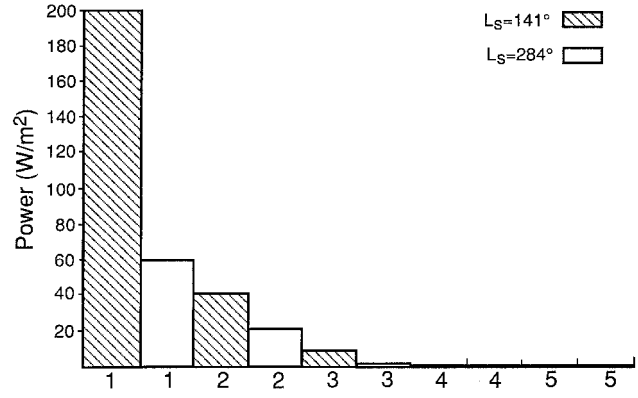

Fig. 14 Radiation loss division of various parts of the PV array.

solar cell temperature along with the variation of the ambient temperature for the summer L_s = 141° and winter L_s = 284°. The maximum temperature for L_s = 141° is 263 K at solar time 12:46, and for L_s = 284° it is 175 K. The variation of the solar cell temperature along the PV array (in the direction of the wind) is shown in Fig. 12 for L_s = 141° and L_s = 284° at VL1, at solar times 11:00 and 12:00, respectively. For L_s = 141°, the difference in temperature is 7.2 deg between the lower and upper edges of the inclined (β = 22.3 deg) PV array; for L_s = 284° the difference is 4.1 deg. The temperature gradient across the PV array layers is negligible.

Figure 13 shows the division of the heat balance equation components of the PV array for L_s = 141° and L_s = 284° at 12:00 solar time. The dark columns represent the solar irradiance absorbed in the PV array (for L_s = 141° and L_s = 284°, respectively), and the other columns are radiation losses, PV array electrical output power, convection losses, and the increase in the energy content of the array. For L_s = 141°, 74% of the solar irradiance absorbed in the PV array are radiation losses. For summer days, the convection losses are no more than 3.9%, whereas in winter, the convection losses may be about 8.6%.

Because the major part of the heat loss mechanism is radiation, the radiation loss division of the various parts of the PV array is shown in Fig. 14 for L_s = 141° and L_s = 284° at 12:00 solar hours. The numbers represent 1) losses to the sky from the front-side; 2) losses to the shadowed ground from the back-side; 3) losses to the sky from the back-side; 4) losses to the ground from the back-side; and 5) losses to the ground from the front-side. The distribution of the losses in the heat balance equation may suggest the use of an approximate formulation of the heat balance equation for determination of the operating solar cell temperature, without resorting to elaborate calculations and data that are hard to obtain. This is outlined in the next section.

V. Discussion

In certain cases, we would like to estimate the operating temperature of the PV array on Mars. So far, we do not have enough data required for the solution of the heat balance equation for all periods and locations on Mars.[15] Therefore, simplified solutions are desirable. Two simplified solutions are described based on the conclusions for the exact solution of the heat balance equation of the three-layer PV array.

1) Neglecting both the free and forced convection heat loss: Line 1 in Fig. 15 describes the solar cell operating temperature using the exact solution of the heat balance equation for L_s = 141° at VL1, and line 2 is the temperature when the convection heat loss is neglected. For winter periods, the difference may be somewhat larger.

2) Simplified heat balance equation: The assumptions are the PV array may be treated as a lumped system for the heat balance equation; radiation heat loss from the PV array to the ground may be neglected; assuming T_{sky} = 0 K, this assumption

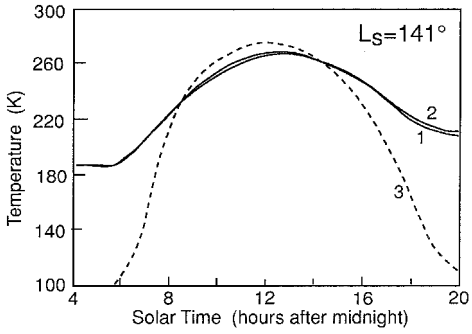

Fig. 15 Solar cell operating temperature.

is based on the large difference between the solar cell and the sky temperatures, and because the temperatures are raised to the power of 4, the heat absorption body (sky) becomes less significant in the heat balance equation. The radiation heat loss from the back-side of the PV array to the shadowed ground is negligible.

Incorporating the preceding assumptions into Eqs. (7), the simplified heat-balance equation becomes

$$mc_p \frac{dT_{cell}}{dt} = \alpha_f G_b \cos\theta + \alpha_f F^f_d G_{dh} - \varepsilon_f \sigma F^f_{sky} T^4_{cell} - Q_p \tag{18}$$

The solution of the solar cell temperature based on Eq. (18) and the values in Fig. 15 are m, 1.56 kg/m^2; c_p, 676 J kg^{-1} K^{-1}; α_f, 0.64; ε_f, 0.86; β, 22.3 deg; latitude ϕ, 22.3°N; and L_s, 141°. During daylight hours, when the solar radiation is relatively high, this solution approximates quite well the exact solution (line 1) of the heat balance equation. It should be emphasized that, except for solar radiation, the approximate solution does not require the climatic data of Mars.

VI. Conclusions

The operating temperature of the solar cells in the flexible PV array was determined from the solution of the heat balance equation consisting of radiation, free and forced convection, and conduction. The PV array was divided into three layers for which three differential equations were obtained and solved. Because the atmosphere and temperatures prevailing on Mars are different from that on Earth, it is necessary to calculate many parameters and coefficients to solve the heat-balance equation. Many of these values are based on Viking Landers measurements and research done on Mars. We believe that this study deals with, for the first time, the detailed formulation and solution of the heat balance equation for Mars.

The main conclusions regarding the formulation of the heat balance equation for the flexible PV array are as follows:

1) Temperature gradients between layers are small, therefore, the PV array may be treated as a lumped system.

2) The convection heat loss is small and the effort required to calculate the various coefficients may not be justified.

3) The radiation heat loss from PV array front- and back-sides to the ground is small and may be neglected.

4) The radiation heat loss from the back-side to the shadowed ground under the array is appreciable.

Acknowledgments

This work was funded under NASA Grant NAGW-2022. We are very grateful to Robert M. Haberle from the Theoretical Studies Branch, NASA Ames Research Center, for supplying us with the data on Surface Heat Balance Tables for Mars. The data sets on Viking Landers ambient temperature, wind speed, and direction and atmospheric pressure used in this research were supplied by Steve Lee, Laboratory for Atmospheric and Space Physics, University of Colorado, Boulder, Colorado.

References

[1]Appelbaum, J., and Flood, D. J., "Solar Radiation on Mars," *Solar Energy*, Vol. 45, No. 6, 1990, pp. 353–363.

[2]Appelbaum, J., Landis, G. A., and Sherman, I., "Solar Radiation on Mars-Update 1991," *Solar Energy*, Vol. 50, No. 1, 1993, pp. 35–51.

[3]Appelbaum, J., Sherman, I., and Landis, G. A., "Solar Radiation on Mars: Stationary Photovoltaic Array," *Journal of Propulsion and Power*, Vol. 12, No. 2, 1996, pp. 410–419.

[4]Ingersoll, J. G., "Simplified Calculation of Solar Cell Temperature in Terrestrial Photovoltaic Arrays," *Journal of Solar Energy Engineering*, Vol. 108, May 1986, pp. 95–101.

[5]Fuentes, M. K., "A Simplified Thermal Model for Flat-Plate PV Arrays," Sandia National Labs., SAND85-0330, Albuquerque, NM, May 1987.

[6]Minning, C. P., *Thermal and Optical Performance of Encapsulation System for Flat-Plate PV Modules*, Jet Propulsion Lab., California Inst. of Technology, Pasadena, CA, 1981, pp. 750–755.

[7]Lillington, D. R., Kukulka, J. R., Mason, A. V., Sater, B. L., and Sanchez, J., "Optimization of Silicon 8 cm × 8 cm Wrapthrough Space Station Cells for on Orbit Operation," *20th IEEE Photovoltaic Specialists Conference* (Las Vegas, NV), Inst. of Electrical and Electronics Engineers, New York, 1988, pp. 934–939.

[8]Duffie, J. A., and Beckman, W. A., *Solar Engineering of Thermal Processes,* Wiley, New York, 1980.

[9]Haberle, R. M., and Jakosky, B. M., "Atmospheric Effects on the Remote Determination of Thermal Inertia on Mars," *Icarus, International Journal of the Solar System*, Vol. 90, No. 2, 1991, pp. 187–204.

[10]Kieffer, H. H., "Soil and Surface Temperature at the Viking Landing Sites," *Science*, Vol. 194, No. 4271, 1976, pp. 1344–1346.

[11]Shorthill, R. W., The Viking Footpad Temperature Sensor," Geospace Sciences Publication 81-014, Salt Lake City, UT, July 1982.

[12]Murphy, J. R., Leovy, C. B., and Tillman, J. E., "Observation of Martian Surface Winds at the Viking Lander 1 Site," *Journal of Geophysical Research*, Vol. 95, No. B9, 1990, pp. 14,555–14,576.

[13]Chapman, A. J., *Heat Transfer*, Macmillan, New York, 1984.

[14]Hendricks, R. C., Baron, A. K., and Peller, I. C., "GASP—A Computer Code for Calculating the Thermodynamic and Transport Properties for Ten Fluids," NASA TN D-7808, Feb. 1975.

[15]Planetary Data System [PDS data set "VLI-M-MET-4-BINNED-P-T-V-CORR-VI.O" and "VLI-IVL2 MARS" Meteorological Research Data], PDS Planetary Atmosphere Discipline Node, Jet Propulsion Lab., Pasadena, CA, 1997.